0026-895X/94/020212-09$03.00/0

MOLECULAR PHARMACOLOGY, 45:212-220

Homomers of α8 and α7 Subunits of Nicotinic Receptors Exhibit Similar Channel but Contrasting Binding Site Properties

V. GERZANICH, R. ANAND, and J. LINDSTROM

Department of Neuroscience, University of Pennsylvania, Philadelphia, Pennsylvania 19104-6074

Received October 18, 1993; Accepted November 29, 1993

SUMMARY

α8 subunits of α-bungarotoxin-sensitive chick neuronal nicotinic acetylcholine receptors expressed in *Xenopus* oocytes from cRNA are shown to form homomeric, acetylcholine-gated, rapidly desensitizing, inwardly rectifying, Ca^{2+}-permeable cation channels similar to those of α7 homomers. α8 forms oligomers of several sizes, of which <14% are expressed on the oocyte surface, which is less efficient than for α7 homomers. α8 homomers are more sensitive to agonists but less sensitive to antagonists than are α7 homomers, and some agonists for α8 homomers are partial agonists or antagonists for α7 homomers. The pharmacological properties of homomers of α8 and α7 subunits generally reflect those of native α8 and α7 receptors.

Two cDNAs for subunits of neuronal nicotinic AChRs that bind αBgt were initially isolated from a chick brain library by Schoepfer *et al.* (1) and termed αBgt-binding protein subunits α1 and α2. These are now termed α7 and α8. These subunits share 62% sequence identity but exhibit <50% identity with other AChR α subunits. Couturier *et al.* (2) showed that α7 formed ACh-gated homomeric cation channels when cRNA for the subunit was injected into *Xenopus* oocytes, but until now expression of α8 cDNA has not been reported.

Three subtypes of neuronal αBgt-binding AChRs have been identified in extracts of brain and retina, 1) α7 AChRs, which contain α7 subunits and are the predominant subtype found in chick brain, 2) α8 AChRs, which contain α8 subunits and are the predominant subtype found in chick retina, and 3) α7α8 AChRs, which contain both α7 and α8 subunits and are a minor subtype in both brain and retina (1, 3). All three subtypes may contain structural subunits that have not been characterized and they do not include characterized structural subunits present in other neuronal AChRs. Purified preparations of αBgt-binding neuronal AChRs have been observed to contain more than a single protein component, but the complete subunit composition of any subtype of αBgt-binding AChR remains unknown (4–7). α8 AChRs have lower affinity for αBgt than do α7 AChRs (3), whereas α8 AChRs have higher affinity for small cholinergic ligands than do α7 AChRs (8, 9). α7 and α8 subunits have been immunohistochemically localized in both chick brain and retina (3, 10–12).

The unique ability of α7 subunits to form functional homomeric channels stimulated intensive studies involving site-directed mutagenesis, which revealed amino acid residues important for ligand binding, activation, desensitization, and ion selectivity of the channel (13–18). The α7 homomer response to agonists in oocytes is characterized by 1) rapid desensitization, 2) high permeability to Ca^{2+}, 3) activation of a Ca^{2+}-dependent Cl^- current, 4) strong rectification, and 5) inhibition by nanomolar αBgt (2, 19, 20).

Here we show that α8 homomers can be studied electrophysiologically, even though they are expressed on the oocyte surface less efficiently than are α7 homomers. The low efficiency of α8 homomer expression on the surface probably reflects a greater dependence on structural subunits of the kind that are indispensable for efficient surface expression of AChR subunits other than α7. α8 homomers, like α7 homomers, desensitize rapidly, exhibit inward rectification, and are highly permeable to Ca^{2+} ions, which trigger Ca^{2+}-activated Cl^- channels. However, unlike α7 homomers, α8 homomers exhibit lower affinity for αBgt but higher affinity for nicotinic agonists. Although the electrophysiological properties of native α7 and α8 AChRs remain to be determined, both the affinities and the efficacies of ligands for α7 and α8 homomers reflect the ligand-binding properties of native α7 and α8 AChRs.

R.A. is currently supported in part by a National Research Service Award. Research in the laboratory of J.L. is supported by grants from the National Institutes of Health (NS11323), the Muscular Dystrophy Association, the Council for Tobacco Research, USA, Inc., and the Smokeless Tobacco Research Council, Inc.

ABBREVIATIONS: AChR, acetylcholine receptor; αBgt, α-bungarotoxin; BAPTA, 1,2-bis(*O*-aminophenoxy)ethane-*N*,*N*,*N*′,*N*′-tetraacetic acid; DMPP, 1,1-dimethyl-4-phenylpiperazinium; mAb, monoclonal antibody; TMA, tetramethylammonium; AM, acetoxymethyl ester; NMDA, *N*-methyl-D-aspartate; SDS, sodium dodecyl sulfate; HEPES, 4-(2-hydroxyethyl)-1-piperazineethanesulfonic acid; EGTA, ethylene glycol bis(β-aminoethyl ether)-*N*,*N*,*N*′,*N*′-tetraacetic acid.

Materials and Methods

mAbs. mAbs to α7 (318) and to α8 (305) have been described previously (1). The epitope for mAb 318 was mapped to within α7 residues 380–400, using synthetic peptides, whereas mAb 305 binding was found to depend on the native conformation of α8 (21). The mAbs were affinity purified using Protein G-agarose.

Expression of α7 and α8 subunits in oocytes. The chicken α7 and α8 cDNAs were cloned into a modified SP64T expression vector (22), using standard DNA cloning procedures. cRNA was synthesized *in vitro* using a standard protocol (22) and more recently using the Megascript kit (Ambion, Austin, TX). Oocytes were prepared for injections as described by Colman (23) and were injected with either ~15 ng or 100 ng of cRNA per oocyte. The oocytes were incubated under semisterile conditions at 18°, in saline solution (96 mM NaCl, 2 mM KCl, 1 mM $MgCl_2$, 1.8 mM $CaCl_2$, 5 mM HEPES, pH 7.6) containing 5% heat-inactivated horse serum, for 3–4 days before use. Metabolic labeling of expressed α8 subunits was achieved by incubating injected oocytes for 3–4 days in saline solution containing 0.5 mCi/ml [^{35}S] methionine (~1000 Ci/mmol; Amersham).

Surface expression was determined by incubating oocytes with 100 nM ^{125}I-αBgt for 2 hr in normal saline solution containing 10% horse serum, followed by five 1-ml washes with normal saline solution. Total expression was determined in the presence of 50 nM ^{125}I-αBgt, using Triton X-100 extracts of oocytes in solid-phase radioimmunoassays on Immulon 4 wells coated with mAb 305.

Solubilization and sucrose gradient analysis of AChRs from oocytes. Oocytes expressing α8 subunits were homogenized in lysis buffer (2% Triton X-100, 50 mM NaCl, 50 mM sodium phosphate, pH 7.5, 5 mM EDTA, 5 mM EGTA, 2 mM phenylmethylsulfonyl fluoride, 5 mM benzamidine, 5 mM iodoacetamide, 1 mg/ml heat-denatured bovine serum albumin), incubated at 4° for 30 min, and centrifuged for 10 min in a microfuge to clear the cellular debris. The cleared lysate was then used for all assays. Aliquots (~500 ml) of extracts from 10 oocytes were layered onto 11-ml sucrose gradients (5–20%), as described previously (24), and the sedimentation of AChRs was analyzed by ^{125}I-αBgt binding (at 50 nM) to the protein complexes immunoimmobilized on Immulon 4 microwells coated with mAb 305. Immunoimmobilized [^{35}S]methionine-labeled expressed α8 subunits from the sucrose gradient fractions were eluted from the microwells with sample buffer and electrophoresed on 10% SDS-polyacrylamide gels. The gels were then treated for fluorography, dried, and exposed to X-ray film at −70° for 1–3 days. The gels were aligned with the X-ray films, the gel slices containing the α8 subunits were excised, and the amount of radioactivity in each gel slice was determined by liquid scintillation counting.

Electrophysiological procedures and drug application. Experiments were performed on *Xenopus laevis* oocytes that had been isolated and incubated using conventional methods. Currents were measured using a standard two-microelectrode voltage-clamp amplifier (oocyte clamp OC-725; Warner Instrument Corp.). Electrodes were filled with 3 M KCl and had resistances of 0.5–1.0 MΩ for the voltage electrode and 0.4–0.6 MΩ for the current electrode. All records were digitized and stored on a Gateway PC 486 computer and were analyzed using pCLAMP and AXOGRAPH software (Axon Instruments).

The recording chamber was continually perfused, at a flow rate of 10 ml/min, with saline solution (96 mM NaCl, 2 mM KCl, 1.8 mM $CaCl_2$, 1 mM $MgCl_2$, 5 mM HEPES, pH 7.6). Application of drugs was performed using a set of eight glass tubes (internal diameter, 2 mm) ending in the bath 3 mm from the oocyte and connected to 10-ml syringes that were placed 10 cm above the recording chamber and that contained control and test solutions. Manual unclamping of the flexible tube connecting the syringe with the agonist solution to the perfusion glass tube directed at the oocyte resulted in appearance of current. The delay between the beginning of application (detected as a short inward deflection on some traces, due to a mechanical artifact of unclamping the connecting tube) and the appearance of current was typically 250–300 msec and apparently depended on the time needed for agonist to reach the oocyte. The application was terminated (typically after 2–5 sec) by clamping the connecting flow tube, and then the perfusion solution was effectively changed back to control due to the continuous flow through the recording chamber. The same response was observed when an oocyte was exposed to an agonist by manual lateral movement of the flow tubes, with continuously flowing solutions, from the position in which the mouth of the tube with control solution was directed onto the oocyte to the position in which the oocyte was superfused with solution containing an agonist. The application was terminated by moving the tubes back to the first position. Because of their very slow off rates (tens of minutes), all antagonists except for curare were applied only by perfusion of the recording chamber. Because of its extremely fast off rate, curare was applied by both bath application and addition to solutions containing agonist. Solutions used to test the effects of αBgt also contained bovine serum albumin (100 μg/ml), to minimize adsorption of αBgt to the plastic surfaces. BAPTA/AM ester (Molecular Probes, Inc.) was stored desiccated at −20° as aliquots of a 100 mM solution in dimethylsulfoxide (Sigma). Aliquots were thawed and diluted 1000-fold into saline solution shortly before incubation of the oocytes.

Results

Biochemical characterization of α8 and α7 homomers expressed in oocytes. The fraction of α8 subunits that were expressed on the surface of the oocyte increased with increasing doses of cRNA. Injection of ~15 ng of α7 cRNA typically yielded ~15 fmol of αBgt binding sites/oocyte, of which 40% were on the surface. This is equal to or greater than the 38% of *Torpedo* $(\alpha1)_2\beta1\gamma\delta$ AChRs or 33% of chick $(\alpha4)_2(\beta2)_3$ AChRs expressed on the surface of oocytes injected with 15-ng doses of each subunit cRNA (25).[1] However, 15 ng of α8 cRNA resulted in even more total αBgt binding sites (28 fmol/oocyte) but only 3.6% were on the surface. Increasing the amounts of subunit cRNAs to 100 ng/oocyte did not increase the surface expression of α7 homomers but increased the surface expression of α8 homomers to 14%.

Sucrose gradient sedimentation of α8 subunits expressed in oocytes revealed ^{125}I-αBgt-labeled complexes starting at the size of monomers of *Torpedo* AChRs and extending to larger aggregates (Fig. 1). This contrasts with α7 subunits, where only a single component, of the size of native α7 AChRs and slightly larger than monomers of *Torpedo* AChRs, binds ^{125}I-αBgt (8). Native α7 and α8 AChRs are probably composed of five subunits, as are the $(\alpha1)_2\beta1\gamma\delta$ AChRs of electric organ or the $(\alpha4)_2(\beta2)_3$ AChRs of brain (24). The sedimentation rates of α8 subunit oligomers observed here suggest that most are composed of four α8 subunits or five α8 subunits, with smaller amounts of larger aggregates. It may be that only homomers composed of five subunits properly arranged around a central cation channel as in native AChRs (26) are actually expressed on the surface. We have no direct evidence for this but did observe that, although dose-response curves for surface α8 homomers exhibited the shape expected for a homogeneous population, ^{125}I-αBgt binding to immunoisolated total α8 homomers and ligand inhibition of this binding exhibited broad curves over larger concentration ranges, as might be expected for a heterogeneous population of binding sites (consequently, data not shown). This contrasts with α7 homomers, which exhibit a single αBgt-binding component on sucrose gradients and exhibit both dose-response curves for surface α7 homomers and ligand-binding curves for immunoisolated total α7 homomers with the shape typical of a homogeneous population (8).

[1] Y. Li, V. Gerzanich, and J. Lindstrom, unpublished observations.

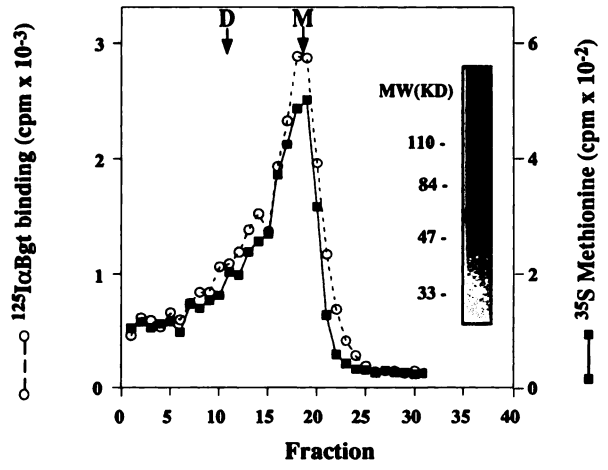

Fig. 1. Sizes of α8 homo-oligomers expressed in *Xenopus* oocytes. This shows the sedimentation profile on a 5–20% sucrose gradient in Triton X-100 of α8 subunits expressed in oocytes injected with 100 ng of cRNA. Binding to the immunoimmobilized protein was measured using 50 nM ^{125}I-αBgt. *Arrows*, position of *Torpedo* AChR monomers (*M*) and dimers (*D*). The [^{35}S]methionine-labeled protein immobilized from the extracts on mAb-coated microwells was then eluted off in sample buffer and subjected to SDS-polyacrylamide gel electrophoresis followed by fluorography. The α8 subunit bands thus identified were excised and the amount of [^{35}S]methionine per fraction was determined by liquid scintillation counting. *Inset*, fluorogram of the [^{35}S]methionine-labeled protein in the lane corresponding to the peak ^{125}I-αBgt binding fraction.

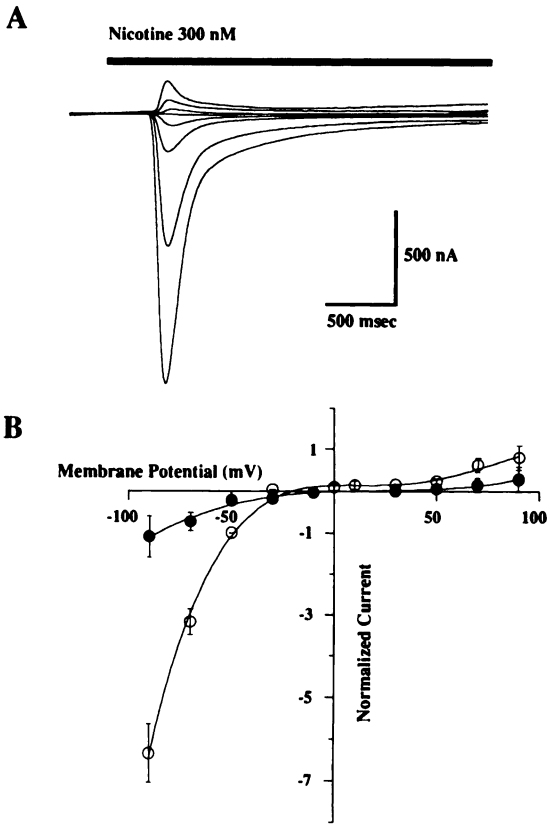

Fig. 2. Inward rectification of α8 homomer-mediated responses. A, This shows the family of currents obtained by application of 0.3 μM nicotine to an oocyte held at different potentials in the range from −90 mV to +70 mV. The difference in holding potential between each *trace* shown is 20 mV. B, The averaged current-voltage relationships of peak currents induced in normal medium (○) (n = 5) and in Ca^{2+}-free medium (●) (n = 3) are plotted. Amplitude of the current at +70 mV was less than that at −70 mV, by 5.2- and 5.3-fold in normal and Ca^{2+}-free medium, respectively. Currents were normalized to the current induced in normal medium in oocytes held at −50 mV.

Metabolic labeling of α8 subunits expressed in oocytes with [^{35}S]methionine, followed by solubilization with Triton X-100, sucrose gradient sedimentation, and immunoisolation, revealed an array of α8 oligomers that closely paralleled the distribution of ^{125}I-αBgt binding (Fig. 1). This contrasts with α7, where there was an even broader distribution of [^{35}S]methionine-labeled oligomers but only the major component (~10 S) bound ^{125}I-αBgt (8). The immunoisolated [^{35}S]methionine-labeled oligomers consisted of only a single subunit, with an apparent molecular weight of ~60,000, as demonstrated by electrophoresis on polyacrylamide gels in SDS and autoradiography. Thus, unless a comigrating endogenous subunit is supplied by the oocyte, it appears that α8 subunits expressed in oocytes form true homomers rather than associating with a *Xenopus* subunit, a possibility for which there is some precedent (27).

Functional characterization of α8 homomers. After 36–48 hr, >90% of oocytes injected with α8 cRNA responded to nicotinic agonists. When 15 ng of cRNA were injected per oocyte, the maximum current amplitude induced by 1 μM nicotine was 200 nA. Increasing the amount of cRNA to 100 ng/oocyte increased currents to a maximum of 10 μA. As illustrated in Fig. 2A, nicotine induces an inward current, which peaks within 100–200 msec and then decays almost to a basal level within <1 sec. The responses were very repeatable upon successive applications and in fact could be repeated within 90 sec if 1 μM nicotine was applied for only 1 sec. In some oocytes α8 homomer responses could be evoked for up to 5 hr without significant run-down.

Voltage dependence of the α8 homomer response. The current-voltage relationship was measured by applying a constant dose of nicotine at different holding potentials (Fig. 2). Depolarization substantially attenuated the peak amplitude. In the range between −20 and +30 mV, strong rectification of the current-voltage curve impaired precise estimation of the reversal potential, which averaged −13.6 ± 3 mV (n = 6). This is close to the reversal potential (−15.3 ± 2.7 mV) of the current through chick α7 homomers expressed in *Xenopus* oocytes in our experiments and to that obtained previously under similar conditions by Galzi *et al.* (16) but is significantly more positive than the reversal potential (−29 mV) observed for rat α7 homomers (20).

Besides clear rectification at potentials around 0 mV, the α8 homomer-mediated response showed unusually strong inward rectification at more negative potentials. The rectification coefficient calculated as the ratio of chord conductances ($G_{-90\ mV}$/$G_{-50\ mV}$) averaged 2.2 ± 0.2 (n = 5).

Desensitization of the α8 homomer response. Increasing concentrations of agonists increased the rates of both the rise and the desensitization of the response (Fig. 3). The time course of recovery from desensitization was estimated using a paired application protocol in experiments where the agonist was applied again at intervals after a control application. Increasing the agonist concentration or duration of application delayed recovery from desensitization. Thus, for saturating concentrations of agonists the interval between applications was increased to 10 min.

High Ca^{2+} permeability of α8 homomers, resulting in

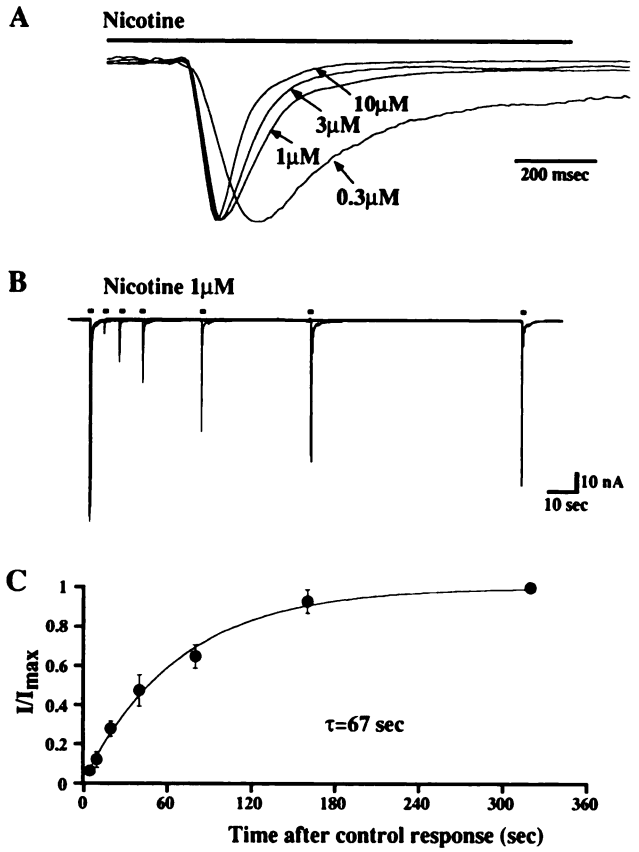

Fig. 3. Desensitization of the α8 homomer-mediated response. A, Increasing nicotine concentrations resulted in acceleration of both the rise and the desensitization of the response. Nicotine was applied at four different concentrations and the corresponding currents were normalized and superimposed. The time constant (τ) for the monoexponential fit of decay of the current induced by 1 μM nicotine was 0.11 sec (average, 0.13 ± 0.02 sec, $n = 5$). B, Primary data for recovery from desensitization are shown. Each of five superimposed traces starts with a 2-sec application of 1 μM nicotine, followed by a second application at a later time. The holding potential in A and B is −20 mV, to prevent contamination by the Ca^{2+}-dependent Cl^- current. C, The time course of recovery from desensitization is plotted. The graph represents averaged data from three experiments, one of which is illustrated in B. Data points are fitted by a single-exponential curve with a time constant of 67 ± 0.5 sec.

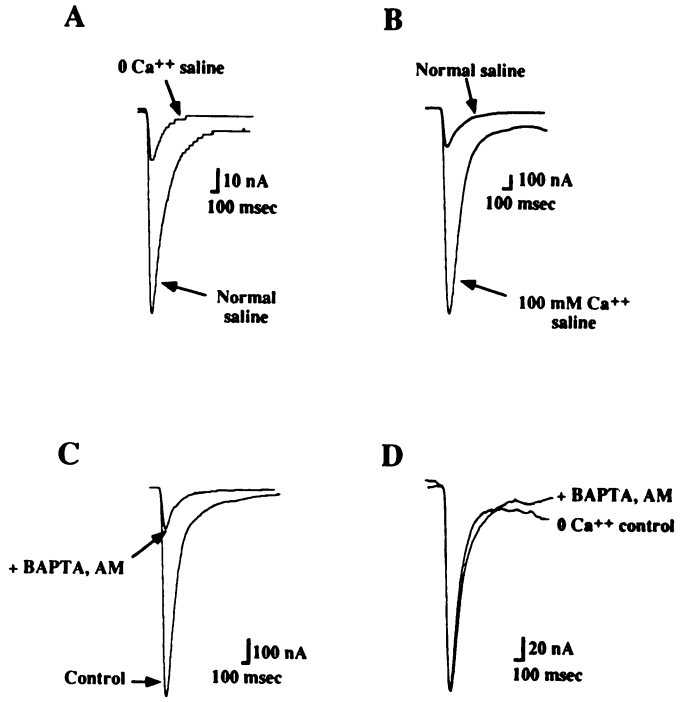

Fig. 4. Evidence that Ca^{2+} permeating through α8 homomers triggers a large endogenous Ca^{2+}-dependent Cl^- current. A, Currents induced by application of 1 μM nicotine in normal saline solution and in saline solution depleted of Ca^{2+} ions (5 mM EGTA was added to avoid possible Ca^{2+} contamination) at a holding potential of −70 mV are shown. Triggering of a secondary endogenous Ca^{2+}-dependent Cl^- current was prevented in Ca^{2+}-free solution. B, Current obtained in normal saline solution is compared with current induced when Na^+ was substituted by Ca^{2+}. *Traces* shown in A and B were obtained in the same experiment. Ca^{2+} permeated through α8 homomers and triggered a large endogenous Ca^{2+}-dependent Cl^- current. C, Currents induced in normal saline solution before and after a 30-min incubation of the oocyte with 100 μM BAPTA/AM are compared. BAPTA/AM permeated into the cytoplasm and, after hydrolysis, chelated Ca^{2+} ions that entered through α8 homomers. This eliminated the secondary Ca^{2+}-dependent Cl^- current. D, Currents induced in Ca^{2+}-depleted extracellular solution before and after incubation of the oocyte with BAPTA/AM are compared. Incubation in BAPTA/AM did not influence the function of the α8 homomer itself. All currents shown in A, B, C, and D were induced by application of 0.3 μM nicotine for 2 sec to oocytes voltage-clamped at −70 mV.

triggering of a Ca^{2+}-dependent Cl^- channel. α7 homomers expressed in oocytes are highly permeable to Ca^{2+} ions (16, 20). The M2 sequence, which is generally accepted as forming part of the channel and contributing to regulation of ion permeability in AChR subunits, is identical in α7 and α8 subunits (1). Thus, it was expected that the ion selectivity of the α8 and α7 homomers should be similar or identical.

A substantial fraction of the total current through α8 homomers is carried by Ca^{2+}, and this Ca^{2+} is responsible for triggering Ca^{2+}-sensitive Cl^- channels that account for much of the total current through oocyte membranes in response to activation of α8 homomers. An endogenous Ca^{2+}-dependent Cl^- channel is known to be present in oocytes (28, 29). Activation of this channel has been previously described for some other AChR subtypes (16, 20, 30), as well as for NMDA receptors (31, 32), which are also highly permeable to Ca^{2+}. The role of the Ca^{2+}-sensitive Cl^- channel in the responses obtained with α7 homomers was not recognized in the early publications regarding α7 but is now being realized (16, 19). Fig. 4A shows that the current induced by application of nicotine to an oocyte expressing α8 homomers was dramatically reduced if the solution lacked Ca^{2+} ions. This revealed that the actual cationic current through α8 homomers was only 18 ± 2% ($n = 8$) of the current in a control solution containing 1.8 mM Ca^{2+}. The reversal potential of the α8 homomer-mediated current induced in Ca^{2+}-free extracellular solution was −1 ± 0.6 mV ($n = 5$). The presence of a secondary Cl^- conductance triggered in the presence of Ca^{2+} in the normal saline solution shifted the reversal potential of the α8 homomer-mediated response to −13.6 mV. The reversal potential for the Ca^{2+}-dependent Cl^- channel in *Xenopus* oocytes under similar conditions is about −20 mV (28).

The rectification coefficient ($G_{-90\ mV}/G_{-50\ mV}$) for α8 homomer-mediated currents in Ca^{2+}-free medium was 2.0 ± 0.3 ($n = 5$), close to the value obtained in normal saline solution. Thus, the strong inward rectification and steepness of the I-V curve at negative potentials observed for α8 homomer-mediated currents induced in normal and Ca^{2+}-free media (Fig. 2B) are intrinsic properties of α8 and are not due to the secondary involvement of the Ca^{2+}-dependent Cl^- conductance.

Currents induced in Ca^{2+}-free medium decayed faster than those in normal saline solution. The fast component of current induced by application of 1 μM nicotine in normal saline solution decayed with a τ_1 of 0.18 ± 0.02 sec (n = 5), and in Ca^{2+}-free saline solution the τ_1 was 0.10 ± 0.02 sec (n = 4). The possibility that the acceleration of the current decay in Ca^{2+}-free medium was due to the absence of positive modulation by extracellular Ca^{2+} ions in normal saline solution was ruled out, because the same acceleration of current was observed when the response was induced in normal saline solution at −20 mV (Fig. 3A). This potential is close to the reversal potential of Cl^- current in oocytes, which minimizes the input of Ca^{2+}-dependent Cl^- current to the response. Thus, the secondary Ca^{2+}-dependent Cl^- current induced by Ca^{2+} influx through the α8 homomers not only dramatically increased the current amplitude but also significantly increased the duration of the response.

When extracellular monovalent cations were replaced with Ca^{2+}, nicotine application resulted in an inward current 570 ± 90% (n = 8) larger than that recorded in normal saline solution, due to increased activation of the Ca^{2+}-dependent Cl^- current (Fig. 4B). The reversal potential of the current induced under this condition (−21 ± 2.5 mV, n = 6) was close to the −20-mV reversal potential of the Cl^- current.

To further establish the mechanism of dependence of the α8 homomer-mediated response on extracellular Ca^{2+}, we chelated intracellular Ca^{2+} using BAPTA. To deliver BAPTA inside the cell we used its permeable ester, BAPTA/AM, which is hydrolyzed to the active Ca^{2+} chelator BAPTA by cytoplasmic enzymes (33). The effectiveness of BAPTA/AM in chelating intracellular Ca^{2+} ions was verified by its ability to block the Ca^{2+}-dependent Cl^- current triggered by Ca^{2+} release from intracellular stores. Miledi and Parker (34) showed that release from intracellular stores can be stimulated through activation of inositol trisphosphate by incubation of oocytes in solutions containing horse serum. In our experiments also, bath application of 5% horse serum induced large (up to 2 μA) chloride currents that reversed around −20 mV, and these were completely blocked by incubation with 100 μM BAPTA/AM.

Incubation in BAPTA/AM resulted in dramatic attenuation of the currents induced by 1 μM nicotine (to only 23 ± 3% of control, n = 5) (Fig. 4C) and the reversal potential was shifted to −2 ± 1.6 mV. These values approximate those measured in Ca^{2+}-free medium. Thus, BAPTA/AM appeared to be very effective in chelating intracellular Ca^{2+} ions.

In the absence of external Ca^{2+}, BAPTA/AM had no effect on the response, indicating that the presence of BAPTA inside the cell did not affect the function of the α8 homomer itself (Fig. 4D). However, in the absence of external Ca^{2+} chelation of intracellular Ca^{2+} ions by BAPTA showed the kinetics by increasing the fast component (τ_1) of current decay from 0.10 ± 0.02 sec to 0.19 ± 0.04 sec (n = 4), suggesting that desensitization of α8 might be modulated by intracellular Ca^{2+} (35). This change in the current kinetics reflects properties of the α8 channel itself. No secondary current is triggered in Ca^{2+}-free medium.

Pharmacological comparison of α8 and α7 homomers. α8 homomers were much more sensitive to agonists than were α7 homomers (Fig. 5; Table 1). Agonist dose-response curves were fitted using a nonlinear Hill equation. Hill coefficients for α8 homomers were >1, except for cytisine, for which the value

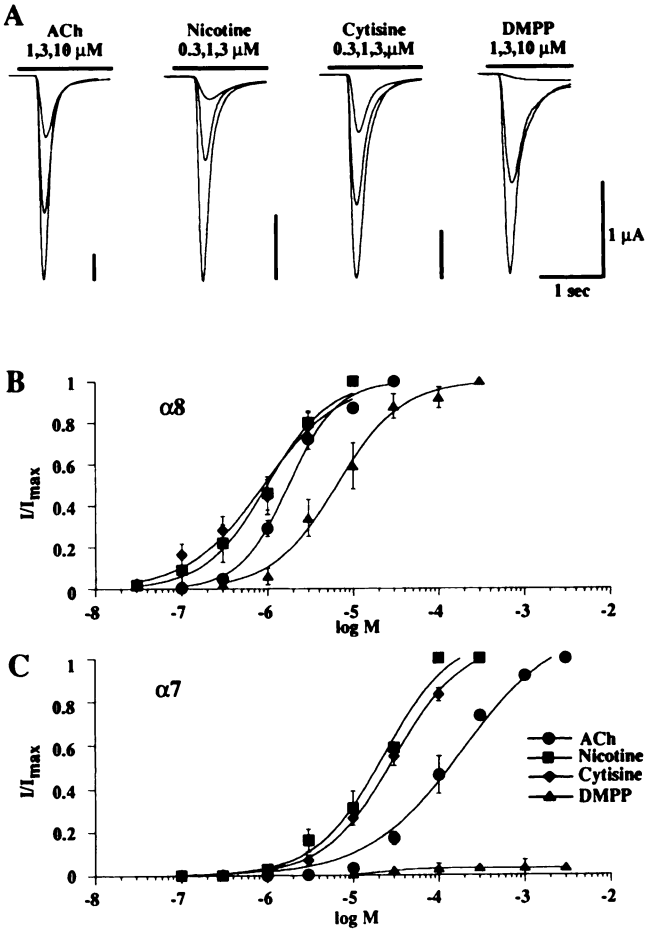

Fig. 5. Comparison of the effectiveness of agonists on α8 and α7 homomers. A, Typical responses induced by ACh, nicotine, cytisine, and DMPP in oocytes expressing α8 homomers are shown. Concentrations of agonists are shown *above the traces*. Data are from different oocytes and currents were normalized to indicate that all tested compounds behaved as full agonists. Oocytes were voltage-clamped at −70 mV. All *vertical bars* in the calibrations are 1 μA. B, Agonist dose-response curves from oocytes expressing α8 homomers are shown. Experimental data were fitted by the Hill equation. C, Agonist dose-response curves from oocytes expressing α7 homomers are shown. The maximum response induced by DMPP was normalized to the maximum response induced by nicotine in the same oocyte. Each *point* in B and C was averaged from three to seven experiments (mean ± standard error).

was 1. The steepness of the dose-response curves was apparently attenuated due to desensitization of the response at high concentrations. A more accurate estimation of Hill coefficients was possible from dose-response curves using only low concentrations of agonists (Table 1). Values greater than 1 indicate that more than one molecule of agonist has to bind to an α8 homomer for the channel to open. α8 homomers showed approximately the same high sensitivity to the nicotinic agonists nicotine, cytisine, and ACh, while exhibiting lower sensitivity to DMPP or TMA. Unlike α8 homomers, α7 homomers were much less sensitive to ACh than to nicotine. TMA was approximately 80 times more potent with α8 homomers than with α7 homomers.

Some ligands differed not only in apparent affinity but also in efficacy between α8 homomers and α7 homomers (Fig. 5). All agonists tested with α8 homomers behaved as full agonists. DMPP acts as a partial agonist at rat α7 homomers (20) and chick α7 homomers (36). In our experiments DMPP produced

TABLE 1
Comparison of the pharmacology of α8 and α7 homomers expressed in *Xenopus* oocytes and native α8 and α7 AChRs

	α8 homomers		Native α8 AChRs, binding IC_{50}[a]		α7 homomers			Native α7 AChRs, binding IC_{50}[a]
	Functional EC_{50}	n_H	Site 1	Site 2	Functional EC_{50}	n_H	Binding IC_{50}[b]	
	μM		μM		μM		μM	μM
Agonists								
ACh	1.9 ± 0.3	1.8	0.031 ± 0.01	390 ± 120	112 ± 7	1.7	55.5 ± 10	160 ± 26
Nicotine	1.0 ± 0.1	1.5	0.012 ± 0.002	11 ± 5	7.8 ± 3	1.7	1.22 ± 0.04	1.3 ± 0.6
Cytisine	1.0 ± 0.2	1.4	0.035 ± 0.005	0.94 ± 0.14	18 ± 2	1.4	0.17 ± 0.02	2.0 ± 0.1
DMPP[c]	6.5 ± 0.6	1.6	0.39 ± 0.09	26 ± 15	30 ± 3	1.4	ND[d]	83 ± 6.0
TMA	10 ± 0.3	1.5	8.0 ± 1.0	700 ± 360	800 ± 200	1.6	22.3 ± 4.2	400 ± 110
Antagonists								
αBgt	0.0014 ± 0.0003	1.6	0.0224 ± 0.0010	ND	0.00030 ± 0.00020	1.3	0.00160 ± 0.00008	0.0019 ± 0.0002
Curare	0.6 ± 0.2	0.9	0.79 ± 0.24	65 ± 28	0.14 ± 0.02	1.6	11.1 ± 1.0	7.3 ± 2.0
Atropine	0.4 ± 0.06	0.6	0.58 ± 0.12	53 ± 22	7.1 ± 0.5	0.8	330 ± 110	120 ± 12
Strychnine	0.8 ± 0.1	0.6	2.0 ± 0.4	18 ± 12	0.52 ± 0.03	1.3	15.3 ± 1.0	9.9 ± 0.4

[a] From Ref. 9.
[b] From Ref. 8.
[c] Poor partial agonist for α7 homomers.
[d] ND, not determined.

a maximum response only about 3.5% of the maximum response induced by ACh, whereas DMPP was a full agonist with α8 homomers.

Sensitivity of α8 and α7 homomers to the agonists was studied on oocytes held at −70 mV. As shown above, at this potential responses are highly contaminated by the secondary Ca^{2+}-dependent Cl^- current. Dose-response curves for nicotine were also determined for α8 and α7 homomers with the oocytes held at −20 mV, a potential at which contamination by secondary Ca^{2+}-dependent Cl^- current was minimal. Importantly, at this holding potential neither the EC_{50} values nor the slopes differed significantly from those obtained at −70 mV, which indicated that the secondary Cl^- current is proportional to activation of the α8 homomers.

α8 homomers were less sensitive to antagonists than were α7 homomers (Fig. 6; Table 1). αBgt exhibited lower apparent affinity for α8 homomers than for α7 homomers, paralleling the lower affinity of αBgt for native α8 AChRs, compared with native α7 AChRs. Surprisingly, α8 homomers showed virtually the same sensitivity to the classical nicotinic antagonist curare, to the classical muscarinic antagonist atropine, and to strychnine, a classical blocker of central glycine receptors. α7 homomers were also antagonized by all three ligands but were more sensitive to curare.

Discussion

In the present study we have shown that the α8 subunit, which belongs to a family of αBgt-binding proteins, forms functional homomers in the absence of other subunits when expressed in *Xenopus* oocytes. This ligand-activated cation channel displays electrophysiological properties distinct from those of other neuronal AChRs and similar to the electrophysiological properties of its close and better characterized relative, the α7 homomeric channel. Similarity in the behavior of α8 and α7 subunits is expected due to the high overall homology of these proteins (1) and due to the identical amino acid sequences of their M2 transmembrane domains, which are thought to be responsible for lining the cation channel. However, α8 homomers differ significantly from α7 homomers in the lower efficiency with which the α8 subunits assemble and are expressed on the oocyte surface and in the affinity and efficacy of several ligands.

α8 homomers assemble into complexes with sizes expected of tetramers, pentamers, and larger aggregates, all of which can bind αBgt (Fig. 1), whereas α7 homomers also assemble into aggregates of various sizes but only those of the size of native α7 AChRs, probably pentamers, bind αBgt (8). The heterogeneity of the α8 complexes that can bind αBgt precludes ligand binding studies of total immunoisolated protein, in contrast to α7 homomers (8). The low efficiency of expression of α8 homomers on the surface of oocytes impairs detection of their electrophysiological activity, but at high doses of α8 cRNA substantial surface expression is detected. The oligomers expressed on the surface may be selectively pentamers, because dose-response curves, unlike binding curves obtained using total α8 oligomers, are not excessively broad. Whereas ≤14% of α8 is expressed on the surface, 40% of α7 is expressed on the surface, which is as efficient as the expression of the native subunit combinations α1β1γδ or α4β2 (25).[2]

The α8 homomer forms a functional cation channel that, like most other neuronal AChRs, strongly rectifies at potentials close to 0 mV. The reversal potential of the current mediated through this channel is far from the equilibrium potentials of the main cations present in solution, which indicates that the α8 homomers, like other members of the family of nicotinic AChRs, show poor selectivity to cations. However, like α7 (20, 25), the channel formed by α8 subunits exhibits much higher permeability to Ca^{2+} ions than do other nicotinic AChRs. Influx of Ca^{2+} ions through the α8 homomers in oocytes triggers a Ca^{2+}-dependent Cl^- channel. We have distinguished the actual α8 homomer-mediated cation current from the Cl^- current by using an extracellular solution depleted of Ca^{2+} ions and by chelation of intracellular Ca^{2+} with BAPTA. The current through the Cl^- channel forms >80% of the α8 homomer-mediated response in oocytes. The ratio between the α8-mediated cation current and the secondary Cl^- current allows an indirect estimation of the Ca^{2+} permeability of α8 homomers. It appears to be much higher than that through other neuronal AChRs (30), about the same as that of the highly homologous rat and chick α7 homomers (20, 25), and comparable to that of NMDA receptors (31). Strong inward rectification, at least at negative holding potentials, is preserved in α8 homomer-me-

[2] Y. Li, V. Gerzanich, and J. Lindstrom, unpublished observations.

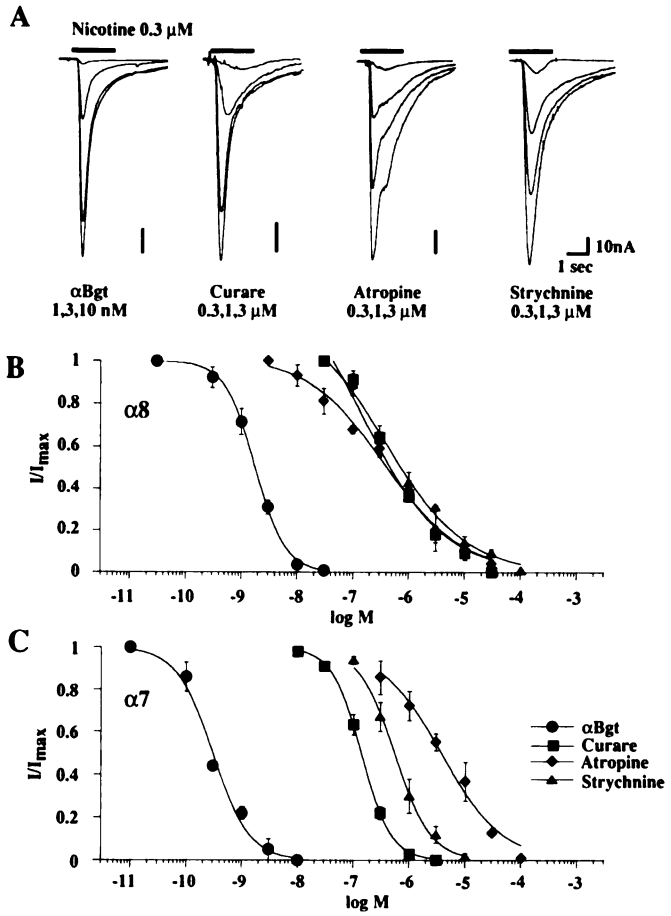

Fig. 6. Comparison of inhibition of $\alpha 8$ and $\alpha 7$ homomer responses by antagonists. A, Inhibition of αBgt, curare, atropine, and strychnine of responses induced by 2-sec application of 0.3 μM nicotine in oocytes with expressed $\alpha 8$ homomers is shown. Oocytes were incubated for 25 min with each concentration of αBgt before application of test nicotine solution. For other antagonists, the incubation time for each concentration was 4–6 min. Responses shown were obtained from different oocytes voltage-clamped at −70 mV. Control responses were normalized. Concentrations of antagonists are shown *below the traces*. B, Antagonist inhibition curves from oocytes expressing $\alpha 8$ homomers are shown. Experimental data were averaged from three to five experiments. C, Antagonist inhibition curves of responses induced by 2-sec applications of 1 μM nicotine from oocytes expressing $\alpha 7$ homomers are shown.

diated responses evoked in Ca^{2+}-free medium, which indicates that the rectification is a genuine property of the $\alpha 8$ homomer and not due to involvement of the secondary Ca^{2+}-dependent Cl^- channel. Interestingly, currents mediated through native αBgt-sensitive AChRs (most likely $\alpha 7$-containing) in chick cochlear hair cells (37, 38) and in rat cultured hippocampal neurons (39, 40) do not show rectification. Because inward rectification is preserved in chick, rat, and human $\alpha 7$ homomers (2, 20, 25, 49),[3] it is possible that structural subunits might be responsible for the absence of rectification in native αBgt-sensitive AChRs.

Responses mediated through the $\alpha 8$ homomers, like those mediated by $\alpha 7$ homomers (2), display unusually fast desensitization. This feature is an intrinsic property of the homomers and is not due to involvement of the secondary Ca^{2+}-dependent Cl^- current, as is the case for responses mediated through NMDA receptors expressed in oocytes (31, 32). Desensitization of the $\alpha 8$ homomer-mediated response persists in Ca^{2+}-free medium and after incubation with the Ca^{2+} chelator BAPTA, AM. Furthermore, inactivation of the endogenous Ca^{2+}-dependent Cl^- current requires tens of seconds (29), which is much slower than the decay of the $\alpha 8$ homomer-mediated responses. Technical limitations (both perfusion of agonist and the large dimensions of oocytes) do not allow simultaneous activation of all homomers on the surface of oocytes. This significantly restricts the resolution of the initial component of desensitization, which is most likely much faster than observed on oocytes under these conditions. On chick cochlear hair cells (37, 38) and on cultured hippocampal neurons (39–41) the native αBgt-sensitive $\alpha 7$-like AChRs undergo extremely fast desensitization, with a current decay time constant in saturating agonist concentrations as fast as 8 msec (41). This strongly suggests that fast desensitization is conserved in native $\alpha 7$- and $\alpha 8$-containing AChRs.

The ability to undergo extremely fast desensitization, together with high Ca^{2+} permeability, makes $\alpha 8$ homomers and $\alpha 7$ homomers, and therefore probably native $\alpha 8$ AChRs and $\alpha 7$ AChRs, unique within the ligand-gated channels family. The response mediated through these AChRs somewhat resembles "Ca^{2+} spikes" mediated through voltage-dependent Ca^{2+} channels. However, unlike voltage-dependent Ca^{2+} channels, these AChRs can provide Ca^{2+} influx at potentials more negative than −50 mV, membrane potentials at which Ca^{2+} channels are inactivated. At these potentials another source of Ca^{2+} influx, NMDA receptors, is also inactivated due to Mg^{2+} block. Fast desensitization and slow recovery from desensitization limit repetitive activation of $\alpha 8$ AChRs and might be involved in regulation of Ca^{2+} entry. AChRs with extremely fast desensitization and high permeability to Ca^{2+} might carry out unique functions under physiological conditions. Ca^{2+} flux through these AChRs might be efficient in triggering secondary currents, for example one mediated through Ca^{2+}-activated K^+ channels. This mechanism is most likely to be responsible for the inhibition mediated through αBgt-sensitive AChRs on chick cochlear hair cells (37, 38) and possibly through αBgt-insensitive AChRs in rat dorsolateral septal neurons (42, 43). $\alpha 7$ AChRs and $\alpha 8$ AChRs may be involved in regulating neuronal process outgrowth through the influx of Ca^{2+}. Lipton *et al.* (44, 45) have described such effects with AChRs on retinal ganglion cells, and αBgt has been shown to similarly regulate process outgrowth in PC12 cells (46).

Pharmacological properties of chick $\alpha 8$ homomers differ significantly from pharmacological properties of chick $\alpha 7$ homomers. Data on $\alpha 7$ homomers obtained in this study confirm results described previously (2, 36). Generally, all the agonists tested appeared to be much more effective in gating $\alpha 8$ homomers, compared with $\alpha 7$ homomers. Surprisingly, ACh, a very low potency agonist for $\alpha 7$ homomers (EC_{50} = 112 μM), displayed high potency for $\alpha 8$ homomers (EC_{50} = 1.9 μM), i.e., close to the potency of nicotine and cytisine. DMPP, a potent full agonist for $\alpha 8$ homomers, appeared to be only an extremely weak partial agonist for chick $\alpha 7$ homomers, although, as shown by Séguéla *et al.* (20), DMPP is more potent in gating rat $\alpha 7$ homomers. However, at concentrations of DMPP higher than 10 μM, Séguéla *et al.* (20) suggested that activation of rat $\alpha 7$ homomers might be combined with open-channel block. The cation channel of AChRs is formed at least in part by the M2 segment of the amino acid sequence of AChR subunits (for review, see Refs. 17 and 47). The M2 segments of chick $\alpha 8$,

chick α7, and rat α7 subunits are completely identical (1, 20). Because DMPP can induce responses with chick α8 homomers at concentrations as high as 300 μM, without any signs of channel block, this mechanism is most likely not responsible for the action of DMPP on chick and rat α7 homomers, where DMPP is a true partial agonist. Striking differences in the action of the nicotinic agonists ACh and DMPP on α8 and α7 homomers are of substantial interest because α8 and α7 subunits share very high (77%) homology in their amino-terminal (putatively extracellular) amino acid sequences (1), which limits the number of amino acids that may be responsible for these differences in affinity and efficacy.

Curare, strychnine, and atropine have similar apparent affinities for α8 homomers; nevertheless, the kinetics of the interaction of these compounds are different. Unlike with curare, which binds and unbinds very fast, beyond the resolution of these experiments, it takes tens of minutes to restore the original response after incubation with strychnine or atropine. Binding experiments with α7 homomers and native α7 AChRs and α8 AChRs show that atropine, curare, and strychnine bind competitively with αBgt (8, 9); however, the differences in the durations of their effects suggest that they may also have noncompetitive antagonistic effects at additional sites.

Interestingly, these pharmacological differences between α8 and α7 homomers are conserved in native α8 and α7 AChRs immunoisolated from chick retina (9). Apparent affinities of compounds tested in the present study for native α8 and α7 AChRs are listed in Table 1 for ease of comparison. Pharmacological properties of native α8 and α7 AChRs were estimated using competitive binding with ^{125}I-αBgt, which complicates direct comparison with EC_{50} values determined electrophysiologically. However, the order of potencies of agonists for α8 and α7 homomers measured electrophysiologically is paralleled by affinities measured using competitive binding assays for α8 and α7 AChRs.

Native α8 AChRs exhibit two classes of binding sites, the high affinity class of which have significantly higher affinity for most ligands than do α7 AChRs. Pharmacological differences between the high affinity binding site of α8 AChRs and the binding site of native α7 AChRs correlate with differences in the pharmacological properties of the α8 and α7 homomers described in the present study. Thus, ACh, nicotine, and cytisine have roughly the same apparent affinities for α8 homomers, and this pattern is conserved with the native α8 AChRs. However, absolute values of the apparent affinities of these agonists for the native α8 AChRs are 30–100 times higher than those for α8 homomers. α7 homomers are substantially less sensitive to ACh, compared with nicotine and cytisine, and this pattern is conserved not only in the affinities of the α7 homomers estimated by competitive binding but also in the affinities of the native α7 AChRs. The same correlation is observed for antagonists. α8 homomers show approximately the same sensitivity to curare, atropine, and strychnine and this property is conserved in the native α8 AChRs for the high affinity binding site. Differences in the sensitivity of α7 homomers to these antagonists are conserved in the pharmacological properties of α7 homomers and native α7 AChRs estimated by competitive binding.

Generally, α8 homomers show significantly higher affinity for the tested agonists than do α7 homomers, and this property appeared to be conserved in the native α8- and α7-containing AChRs. The similarities of pharmacological profiles of native α8 AChRs and α7 AChRs to properties of α8 homomers and α7 homomers expressed in oocytes suggest that the pharmacological properties of these homomers reflect those of the corresponding native AChRs.

As shown by immunohistochemical studies (3, 10, 12), a prominent role for chick α8 AChRs and α7α8 AChRs appears to be in retina. The results of the present study strongly suggest that these AChRs most likely function as ACh-gated cation channels that desensitize rapidly and that may mediate some of their effects through the influx of Ca^{2+}. Recent studies on cultured rat hippocampal neurons (39–41) and chick cochlear hair cells (37, 38) allow comparison of properties of expressed rat and chick α7 homomers with properties of αBgt-sensitive nicotinic responses observed electrophysiologically on these cells, although the functional roles of these responses remain obscure. Currently, despite substantial proof of involvement of nicotinic mechanisms in retina function (for review, see Ref. 48), electrophysiological studies of properties of AChRs that might be involved are rather limited. The properties of α8 homomers shown here (fast desensitization, inward rectification, Ca^{2+} permeability, and distinct pharmacology) are characteristics that can be used in identification of functional native α8-containing AChRs.

Acknowledgments

We thank John Cooper for iodinations, Lorie Criswell for mAb purifications, Michael Katz and Dore Wong for technical assistance, Dawn McCullough for preparation of this manuscript, and all other members of the laboratory for comments on the manuscript.

References

1. Schoepfer, R., W. G. Conroy, P. Whiting, M. Gore, and J. Lindstrom. Brain α-bungarotoxin binding protein cDNAs and mAbs reveal subtypes of this branch of the ligand-gated ion channel gene superfamily. *Neuron* 5:35–48 (1990).
2. Couturier, S., D. Betrand, J. M. Matter, M. C. Hernandez, S. Bertrand, N. Millar, S. Valera, T. Barkas, and M. Ballivet. A neuronal nicotinic acetylcholine receptor subunit (α7) is developmentally regulated and forms a homooligomeric channel blocked by α-BTX. *Neuron* 5:847–857 (1990).
3. Keyser, K. T., L. R. G. Britto, R. Schoepfer, P. Whiting, J. Cooper, W. Conroy, A. Borozozowska-Prechtl, H. J. Karten, and J. Lindstrom. Three subtypes of α-bungarotoxin-sensitive nicotinic acetylcholine receptors are expressed in chick retina. *J. Neurosci.* 13:442–454 (1993).
4. Conti-Tronconi, B. M., S. M. J. Dunn, E. A. Barnard, J. O. Dolly, F. A. Lai, N. Ray, and M. A. Raftery. Brain and muscle nicotinic acetylcholine receptors are different but homologous proteins. *Proc. Natl. Acad. Sci. USA* 82:5208–5212 (1985).
5. Norman, R. I., F. Mehraban, E. A. Barnard, and J. O. Dolly. Nicotinic acetylcholine receptor from chick optic lobe. *Proc. Natl. Acad. Sci. USA* 79:1321–1326 (1982).
6. Gotti, C., W. Hanke, R. Schlue, M. Moretti, and F. Clementi. A functional α-bungarotoxin receptor is present in chick cerebellum: purification and characterization. *Neuroscience* 50:117–127 (1992).
7. Gotti, C., A. E. Ogando, W. Hanke, R. Schlue, M. Moretti, and F. Clementi. Purification and characterization of an α-bungarotoxin receptor that forms a functional nicotinic channel. *Proc. Natl. Acad. Sci. USA* 88:3258–3268 (1991).
8. Anand, R., X. Peng, and J. Lindstrom.. Homomeric and native α7 acetylcholine receptors exhibit remarkably similar but nonidentical pharmacological properties suggesting that the native receptor is a heteromeric complex. *FEBS Lett.* 327:241–246 (1993).
9. Anand, R., X. Peng, J. Ballesta, and J. Lindstrom. Pharmacological characterization of α-bungarotoxin-sensitive acetylcholine receptors immunoisolated from chick retina: contrasting properties of α7 and α8 subunit-containing subtypes. *Mol. Pharmacol.* 44:1046–1050 (1993).
10. Britto, L. R. G., D. E. Hamassaki-Britto, E. S. Ferre, K. T. Keyser, H. J. Karten, and J. M. Lindstrom. Neurons of the chick brain and retina expressing both α-bungarotoxin-sensitive and α-bungarotoxin-insensitive nicotinic acetylcholine receptors: an immunohistochemical analysis. *Brain Res.* 590:193–200 (1992).
11. Britto, L. R. G., K. T. Keyser, J. M. Lindstrom, and H. J. Karten. Immunohistochemical localization of nicotinic acetylcholine receptor subunits in the mesencephalon and diencephalon of the chick. *J. Comp. Neurol.* 317:325–340 (1992).

12. Hamasaki-Britto, D. E., A. Brozozowska-Prechtl, H. Karten, and J. Lindstrom. Bipolar cells of the chick retina containing α bungarotoxin-sensitive nicotinic acetylcholine receptors. *Visual Neurosci.*, in press (1993).
13. Galzi, J. L., D. Bertrand, A. Devillers-Thiéry, F. Revah, S. Bertrand, and J.-P. Changeux. Functional significance of aromatic amino acids from three peptide loops of the α7 neuronal nicotinic receptor site investigated by site-directed mutagenesis. *FEBS Lett.* **294**:198–202 (1991).
14. Revah, F., D. Bertrand, J. L. Galzi, A. Devillers-Thiery, C. Mulle, N. Hussy, S. Bertrand, M. Ballivet, and J. P. Changeux. Mutations in the channel domain alter desensitization of a neuronal nicotinic receptor. *Nature (Lond.)* **353**:846–849 (1991).
15. Bertrand, D., A. Devillers-Thiéry, F. Revah, J. L. Galzi, N. Hussy, C. Mulle, S. Bertrand, M. Ballivet, and J.-P. Changeux. Unconventional pharmacology of a neuronal nicotinic receptor mutated in the channel domain. *Proc. Natl. Acad. Sci. USA* **89**:1261–1265 (1992).
16. Galzi, J. L., A. Devillers-Thiéry, N. Hussy, S. Bertrand, J. P. Changeux, and D. Bertrand. Mutations in the channel domain of a neuronal nicotinic receptor convert ion selectivity from cationic to anionic. *Nature (Lond.)* **359**:500–505 (1992).
17. Changeux, J.-P., J.-L. Galzi, A. Devillers-Thiéry, and D. Bertrand. The functional architecture of the acetylcholine nicotinic receptor explored by affinity labeling and site-directed mutagenesis. *Q. Rev. Biophys.* **25**:395–432 (1992).
18. Changeux, J.-P., A. Devillers-Thiéry, J. L. Galzi, and D. Bertrand. New mutants to explore nicotinic receptor functions. *Trends Pharmacol. Sci.* **13**:299–301 (1992).
19. Devillers-Thiéry, A., J. L. Galzi, S. Bertrand, J.-P. Changeux, and D. Bertrand. Stratified organization of the nicotinic acetylcholine receptor channel. *Neuro Report* **3**:1001–1004 (1992).
20. Séguéla, P., J. Wadiche, K. Dineley-Miller, J. A. Dani, and J. W. Patrick. Molecular cloning, functional properties, and distribution of rat brain α7: a nicotinic cation channel highly permeable to calcium. *J. Neurosci.* **13**:596–604 (1993).
21. McLane, K. E., X. Wu, J. M. Lindstrom, and B. M. Conti-Tronconi. Epitope mapping of polyclonal and monoclonal antibodies against two α-bungarotoxin binding α-subunits from neuronal nicotinic receptors. *Neuroimmunology* **38**:115–128 (1992).
22. Melton, D., P. Krieg, M. Rebagliati, T. Maniatis, K. Zuin, and M. Green. Efficient *in vitro* synthesis of biologically active RNA and RNA hybridization probes from plasmids containing SP6 promoter. *Nucleic Acids Res.* **12**: 7035–7056 (1984).
23. Colman, A. Translation of eukaryotic messenger RNA in *Xenopus* oocytes, in *Transcription, and Translation, A Practical Approach* (B. D. Hames and S. J. Higgins, eds.). IRL Press, Oxford, UK, 271–302 (1984).
24. Anand, R., W. G. Conroy, R. Schoepfer, P. Whiting, and J. Lindstrom. Neuronal nicotinic acetylcholine receptors expressed in *Xenopus* oocytes have a pentameric quaternary structure. *J. Biol. Chem.* **266**:1192–1198 (1991).
25. Li, Y., V. Gerzanich, R. Anand, and J. Lindstrom. Functional properties of neuronal α7 acetylcholine receptor expressed in *Xenopus* oocytes: a comparison with neuronal $\alpha_4\beta_2$ and electric organ $\alpha_1\beta_1\gamma\delta$ acetylcholine receptors. *Biophys. J.* **64**:A322 (1993).
26. Unwin, N. Nicotinic acetylcholine receptor at 9 Å resolution. *J. Mol. Biol.* **229**:1101–1124 (1993).
27. Buller, A. L., and M. M. White. Functional acetylcholine receptors expressed in *Xenopus* oocytes after injection of *Torpedo* β-, γ-, and δ-subunit RNAs are a consequence of endogenous oocyte gene expression. *Mol. Pharmacol.* **37**:423–428 (1990).
28. Miledi, R., and I. Parker. Chloride current induced by injection of calcium into *Xenopus* oocytes. *J. Physiol. (Lond.)* **357**:173–183 (1984).
29. Boton, R., N. Dascal, B. Gillo, and Y. Lass. Two calcium-activated chloride conductances in *Xenopus laevis* oocytes permeabilized with the ionophore A23187. *J. Physiol. (Lond.)* **408**:511–534 (1989).
30. Vernino, S., M. Amador, C. W. Luetje, J. Patrick, and J. A. Dani. Calcium modulation and high calcium permeability of neuronal nicotinic acetylcholine receptors. *Neuron* **8**:127–134 (1992).
31. Leonard, J. P., and S. R. Kelso. Apparent desensitization of NMDA responses in *Xenopus* oocytes involves calcium-dependent chloride currents. *Neuron* **2**:53–60 (1990).
32. Ishii, T., K. Moriyoshi, H. Sugihara, K. Sakurada, H. Kadotani, M. Yokoi, C. Akazawa, R. Shigemoto, N. Mizuno, M. Masu, and S. Nakanishi. Molecular characterization of the family of the *N*-methyl-D-aspartate receptor subunits. *J. Biol. Chem.* **268**:2836–2843 (1993).
33. Yoshida, S., and S. Plant. A potassium current evoked by growth hormone-releasing hormone in follicular oocytes of *Xenopus laevis*. *J. Physiol. (Lond.)* **443**:651–667 (1991).
34. Miledi, R., and I. Parker. Latencies of membrane currents evoked in *Xenopus* oocytes by receptor activation, inositol trisphosphate and calcium. *J. Physiol. (Lond.)* **415**:189–210 (1989).
35. Miledi, R. Intracellular calcium and desensitization of acetylcholine receptors. *Proc. R. Soc. Lond. B Biol. Sci.* **209**:447–452 (1980).
36. Bertrand, D., S. Bertrand, and M. Ballivet. Pharmacological properties of the homomeric α7 receptor. *Neurosci. Lett.* **146**:87–90 (1992).
37. Fuchs, P. A., and B. W. Murrow. Cholinergic inhibition of short (outer) hair cells of the chick's cochlea. *J. Neurosci.* **12**:800–809 (1992).
38. Fuchs, P. A., and B. W. Murrow. A novel cholinergic receptor mediates inhibition of chick cochlear hair cells. *Proc. R. Soc. Lond. B Biol. Sci.* **248**:35–40 (1992).
39. Alkondon, M., and E. Albuquerque. Initial characterization of the nicotinic acetylcholine receptors in rat hippocampal neurons. *J. Recept. Res.* **11**:1001–1021 (1991).
40. Alkondon, M., and E. Albuquerque. Diversity of nicotinic acetylcholine receptors in rat hippocampal neurons. I. Pharmacological and functional evidence for distinct structural subtypes. *J. Pharmacol. Exp. Ther.* **265**:1455–1473 (1993).
41. Zorumski, C. F., L. L. Thio, K. E. Isenberg, and D. B. Clifford. Nicotinic acetylcholine currents in cultured postnatal rat hippocampal neurons. *Mol. Pharmacol.* 931–936 (1992).
42. Wong, L., and J. P. Gallagher. A direct nicotinic receptor-mediated inhibition recorded intracellulary *in vitro*. *Nature (Lond.)* **341**:439–441 (1989).
43. Wong, L., and J. P. G. Pharmacology of nicotinic receptor-mediated inhibition in rat dorsolateral septal neurones. *J. Physiol. (Lond.)* **436**:325–346 (1991).
44. Lipton, S. A., and S. B. Kater. Neurotransmitter regulation of neuronal outgrowth, plasticity and survival. *Trends Neurosci.* **12**:265–270 (1989).
45. Lipton, S. A., M. P. Frosch, M. D. Phillips, D. L. Tauc, and E. Aizenman. Nicotinic antagonists enhance process outgrowth by rat retinal ganglion cells in culture. *Science (Washington, D. C.)* **239**:1293–1296 (1988).
46. Quik, M., R. Cohen, T. Audhya, and G. Goldstein. Thymopoietin interacts at the *alpha*-bungarotoxin site of and induces process formation in PC12 pheochromocytoma cells. *Neuroscience* **39**:139–150 (1990).
47. Changeux, J.-P. Functional architecture and dynamics of the nicotinic acetylcholine receptor: an allosteric ligand-gated ion channel. *Fidia Res. Found. Neurosci. Award Lect.* **4**:21–168 (1990).
48. Daw, N. W., W. J. Brunken, and D. Parkinson. The function of synaptic transmitters in the retina. *Annu. Rev. Neurosci.* **12**:205–225 (1989).
49. Peng, X., M. Katz, V. Gerzanich, R. Anand, and J. Lindstrom. Human α7 acetylcholine receptor: cloning of the α7 subunit from the SH-SY5Y cell line and determination of pharmacological properties of native receptors and functional α7 hormoners expressed in *Xenopus* oocytes. *Mol. Pharmacol.*, in press (1994).

Send reprint requests to: Jon Lindstrom, 217 Stemmler Hall, 36th St. and Hamilton Walk, Department of Neuroscience, University of Pennsylvania, Philadelphia, PA 19104-6074.